Proceedings of the
International Geometry Center
Vol. 15, no. 1 (2022) pp. 32–49

Flows with minimal number of singularities on the Boy's surface

Alexandr Prishlyak, Luca Di Beo

Abstract. We study flows on the Boy's surface. The Boy's surface is the image of the projective plane under a certain immersion into the three-dimensional Euclidean space. It has a natural stratification consisting of one 0-dimensional stratum (central point), three 1-dimensional strata (loops starting at this point), and four 2-dimensional strata (three of them are disks lying on the same plane as the 1-dimensional strata, and having the loops as boundaries). We found all 342 optimal Morse-Smale flows and all 80 optimal projective Morse-Smale flows on the Boy's surface.

Анотація. Розглядаються потоки на поверхні Боя. Поверхня Боя є зануренням проективної площини в тривимірний евклідів простір. Вона має природну стратифікацію, що складається з одного 0-вимірного страту (центральна точка), трьох одновимврних стратів (петель з початком в цій точці) і чотирьох двовимірних стратів (три з них є дисками, що лежать в одній площині з одновимірними стратами та мають ці петлі як свої межі). Спочатку досліджуються потоки без замкнених траекторій та з однією особливою точкою, що є 0-стратом. Показано, що у такого потоку є принамні одна сепаратриса. Доведено, що існує 18 різних структур потоків з однією сепаратрисою. Далі розглядаються потоки Морса-Смейла на поверхні Боя як на стратифікованій множині без врахування її вкладення в тривимірний простір. Доведено, що на кожному 1-страті існує сингулярна точка. Описано всі можливі (342) структури потоків, у яких 4 особливі точки (0-страт і по одній на кожному 1-страті). В кінці роботи розглядаються потоки Морса-Смейла на проективній площині, які проектуються в потоки на поверхні Боя. Такі потоки з найменшим числом особливостей мають 3 витоки, 3 стоки та 5 сідел. Описані всі можливі 80 строуктур потоків з таким набором особливостей.

2010 Mathematics Subject Classification: 37c10, 37c15, 37c20

UDC 517.956.4

Keywords: Morse flow, Morse-Smale flow, topological equivalence, optimal flow, Boy's surface

Ключові слова: Потік Морса, потік Морса-Смейла, топологоічна еквівалентніс́ь, оптимлальний потік, поверхня Боя

DOI: http://dx.doi.org/10.15673/tmgc.v15i1.2225

Introduction

The Boy's surface is a certain immersion of the real projective plane in the three-dimensional space. It was found by Werner Boy in [2](1901). The famous mathematician David Hilbert made an assignment to Boy to prove that $\mathbb{R}P^2$ could not be immersed in the 3D Euclidean space. As seen, it turned out to be possible, and this way the Boy's surface was discovered.

The first explicit parameterization of the Boy's surface was achieved by Bernard Morin in [11](1978), in which it was used to describe the sphere eversion. Another parameterization was discovered by Rob Kusner and Robert Bryant in [7](1987).

In [4](2009), Sue Goodman and Marek Kossowski showed that the Boy's surface is one of the only two possible immersions of the real projective plane with a single triple point. The advantage of the Boy's surface with respect to the Roman surface, and the cross-cap, is that it has no singularities other than self-intersections, *i.e.* it has no pinch-points.

We consider the Boy's surface as a stratified set. Morse theory is often used to study the topological properties of such sets and manifolds. The main constructions in it are made with the help of gradient vector fields (or flow) of Morse functions. In general position, such vector fields are Morse-Smale vector fields without closed trajectories. As the fewer singularities such vector fields have, then all constructions are simpler. Therefore, it is typical to study the structures of such vector fields with a minimum number of singularities.

The initial developments of the theory go back to [1](1937), when the physicist and mathematician A. Andronov and L. Pontryagin, respectively, considered the system $\dot{x} = v(x)$, where v is a C^1-vector field on the plane. They suggested calling it *rough* if for any sufficiently small perturbation in the C^1-metric, there exists a homeomorphism in the neighborhood of the identity map, which sends orbits of the original system to orbits of the perturbed system. They also established a criteria for roughness, which is a finite number of singular points and periodic orbits, all of which hyperbolic, and no saddle connections.

One of the goals was to generalize the results. In the case of generalizing them to arbitrary oriented surfaces of positive genus, the problem was the appearance of non-closed recurrent trajectories. However, in [10](1939) A. Mayer proved that such trajectories do not exist in structurally stable flows without singularities on the 2-torus.

The topological classification of structural stable flows on a bounded part of the plane, and on the 2-spheres, were accomplished only in [8](1955) by E. Leontovich-Andronova and A. Mayer.

In [14](1959), M. Peixoto generalized the concept of roughness by the introduction of the notion of *structural stability.* A flow f^t is called structurally stable if, for any sufficiently close flow g^t, there exists a homeomorphism h sending orbits of the system g^t to orbits of the system f^t. Hence, the requirement of a homeomorphism in the neighborhood of the identity map (as in the definition of rough system) is relaxed for structurally stable systems.

In [15](1962), M. Peixoto showed that the concepts of structural stability and roughness are equivalent for 2D flows. As a consequence of the generalization of properties of rough flows to orientable surfaces, there arises the concept of *Morse-Smale* systems. In such systems, the non-wandering set consists of finitely many singular points and periodic orbits, each of which is hyperbolic, and the stable and unstable manifolds intersect transversely for any distinct non-wandering points.

Morse-Smale systems received this name after the paper, written by S. Smale, in [27](1960). He presented flows with the corresponding properties on manifolds of dimension greater than 2, and showed that they satisfy inequalities similar to the Morse inequalities, regarding the critical points of a manifold. Only in [13](1979), J. Palis and S. Smale proved that Morse-Smale systems are structurally stable.

In [16](1973) M. Peixoto, and in [12](1998) A. Oshemkov and V. Sharko, and others, achieved a structural classification of Morse-Smale vector fields on closed surfaces.

A Morse-Smale flow without closed orbit is called a *Morse flow.* We say that flow is *optimal* if it has the lowest number of fixed points among all flow of that type on the surface.

The Morse flow on the closed surface is optimal if and only if it has only one sink and one source, according to Z. Kibalko, A. Prishlyak, R. Shchurko in [6](2018). Such a flow is also called a *polar* Morse flow. The topological structure of polar (optimal) Morse flows on closed 2- and 3-manifolds was described in [3, 5, 6, 9, 17, 18, 21].

Morse-Smale flows with singularities on a surface with a boundary was investigated in [20, 22–26].

The formula for the sum of singularities indices is useful for calculating their number for flow on a stratified set [19].

In this paper we unit these two important concepts in mathematics (Boy's surface and Morse-Smale systems) that have being developed since the beginning of the XX century. One of the goals here is to describe topological structures of flows with minimum number of singular trajectories.

Structure of the paper. This paper contains results concerning flows applied to the Boy's surface with minimal number of singularities.

Section 1 contains topological properties of flows on the Boy's surface. We show that 1-strata are invariant with respect to all flows and the 0-stratum is a singular point for every flow on Boy's surface (Lemma 1.1). It was proved that there is at least one separatrix of a flow with the only one fixed point, and there are 18 different structures of such flows with one separatrix (Theorem 1.2).

Section 2 possesses definitions of such flows in a manifold with boundary and in a stratified space. We define Morse-Smale flows in general (Definition 2.1) and on stratified spaces (Definition 2.2), the concept of separatrix in this context (Definition 2.3) and of optimal Morse-Smale (MS-) flows (Definition 2.4). We also prove the following three theorems: (Theorem 2.5) optimal Morse-Smale flows in the Boy's surface do not have closed orbits; (Theorem 2.6) each 1-strata of MS-flows contains at least one fixed point of the flow; (Theorem 2.7) there are 342 topologically nonequivalent optimal MS-flows in the Boy's surface.

Section 3 considers projective MS-flow (PMS-flow), *i.e.* Morse-Smale flows on the real projective plane, which are flows projected on the Boy's surface. We prove Theorem 3.1 that states that there exist 80 optimal PMS-flows in the projective plane, with 3 sources, 5 saddles, and 3 sinks.

1. Single fixed point flows

Let us describe some topological properties of the Boy's surface. The Figure 1.1 is the so-called fundamental (curved) polygon of the Boy's surface [2]. In order to show that, the following two remarks are helpful:

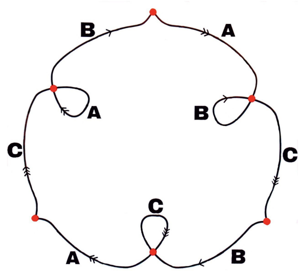

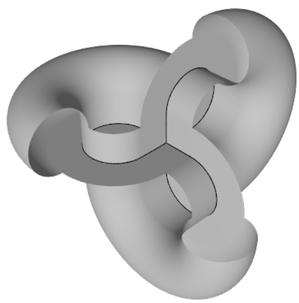

Figure 1.1. Boy's surface as the immersion of the projective plane

(1) opposite sides of the fundamental polygon must be attached in opposite directions in order to capture the non-orientability of the projective plane;
(2) the loops must be attached to the sides, satisfying the orientation shown on the Figure 1.1 left, in order to result in Figure 1.1 right.

Consider the Boy's surface (Figure 1.1 right), which is the immersion of the projective plane in three-dimensional space, and cut it by its 3 loops in order to obtain 4 disks. The loops are the 1-strata, and the disks are the 2-strata.

Since the triple point (0-stratum) is unique, when cutting the 3 loops, 6 copies of the same point are generated (one in each loop and one in each boundary connecting loops – red points in Figure 1.1 left). The corners are the result of the non-smoothness at the triple point, for it is characterized as the intersection of three surfaces. This explains how the proper surgeries performed in the space in Figure 1.1 right yields Figure 1.1 left.

Let us describe the topological properties of flows on Boy's surface.

Lemma 1.1. *On the Boy's surface, if a trajectory passes through a point of a* 1*-stratum, then it belongs to this stratum. Moreover, its* 0*-stratum is a singular point of every flow.*

Proof. Concerning the 1-strata: suppose there are two non-parallel surfaces intersecting along a line, such that in each of them there is a smooth vector field at each point. Figure 1.2 illustrates a simple case, when these surfaces are planes. Each vector belongs to the tangent space at the point on the surface. Hence, for every point on the line of intersection of the surfaces, the vector at this point must be simultaneously tangent to both surfaces. The only way for it to happen is if the tangent vectors at points on the line are tangent to the line itself. This is illustrated in Figure 1.2, where all (red) vectors at points on the red line (1-stratum) are tangent to the red line. This way, the system generates a flow that is invariant in each 1-stratum (see Figure 1.2).

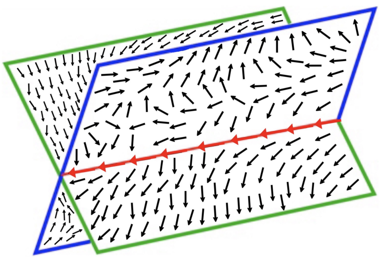

FIGURE 1.2. Vector along the red line of intersection is tangent to the line itself

Now, let's consider the proof about the 0-stratum. As the vector field on the Boy's surface is assumed to be smooth, each of its vectors belong to the tangent space at a point. When such point is a 0-stratum (point of intersection of 3 surfaces), the vector at this point must be tangent to all 3 surfaces simultaneously, which is possible only when this is a zero vector. Therefore, the vector at the 0-stratum is zero for every flow, and consequently the point is singular. In order to visualize it, make a third surface intersecting the two planes in Figure 1.2, crossing the red line. This triple intersection point is the singular 0-stratum point. □

Consider flows with one fixed point being the 0-stratum. It is easy to see that the α- and ω-limit set of each trajectory is the 0-stratum. If this is not so, then, according to the Poincare-Bendixson theorem, there must exist a closed cycle and a second fixed point inside it.

The 1-stratas and the separatrices divide the surface into regions, which we will call *cells*. Each cell is a curved polygon, the vertices of which are fixed points. Since there are no fixed points inside the cell, each trajectory starts and ends at one of the vertices. There are 4 types of vertex angles: *elliptic*, *hyperbolic*, *sources*, *sinks*.

- In a neighborhood of the elliptic point, the vector field is topologically equivalent to the vector field $\{x^3 - 3xy^2, 3x^2y - y^3\}, x \geqslant 0, y \geqslant 0$;
- in the neighborhood of the hyperbolic point it is equivalent to to the vector field $\{x, -y\}, x \geqslant 0, y \geqslant 0$;
- near the source to $\{x, y\}, x \geqslant 0, y \geqslant 0$;
- and near the sink to $\{-x, -y\}, x \geqslant 0, y \geqslant 0$.

Also note that all cells are of two types:

- one of the corners is a source, another corner is a sink, and the rest are hyperbolic (*polar* cell);
- one of the angles is elliptic, and the rest are hyperbolic (*cyclic* cell).

In a polar cell, trajectories start and end at distinct points, whilst in a cyclic cell, the trajectories start and end at the same point. The boundary of the cyclic cell forms a cycle, and the polar one forms two oriented paths that start at the source and end at the sink. Of course, for MS-flows elliptic vertex angles is not allowed, and thus these flows only have polar cells.

Theorem 1.2. *A flow with one fixed point has at least one separatrix. There are* 18 *different structures of such flows with one separatrix.*

Proof. Note that two types of flows are possible:

a) motion along 1 and 0-strata is possible, which defines a regular curve that coincides with the direction of flow on 1-strata (oriented flow),
b) such motion does not exist (non-oriented flow).

Let us enumerate the angles of the central region counterclockwise starting from the angle between the loops with integers from 1 to 9 (see Figure 1.3).

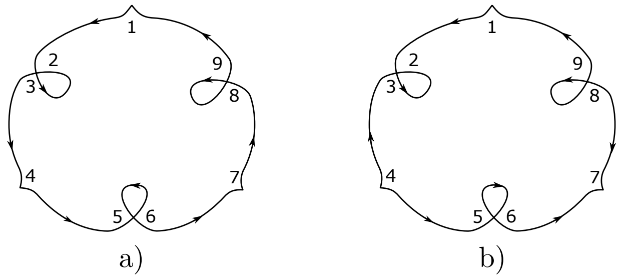

FIGURE 1.3. Oriented (left) and non-oriented (right) flows with one fixed point

In case a) the arcs will be oriented as follows:

$$1 \to 2,\ \ 3 \to 2,\ \ 3 \to 4,\ \ 4 \to 5,\ \ 6 \to 5,\ \ 6 \to 7,\ \ 7 \to 8,\ \ 9 \to 8,\ \ 9 \to 1.$$

In case b) we have the following orientations of the arcs:

$$1 \to 2,\ \ 3 \to 2,\ \ 4 \to 3,\ \ 4 \to 5,\ \ 5 \to 6,\ \ 6 \to 7,\ \ 8 \to 7,\ \ 9 \to 8,\ \ 9 \to 1.$$

In case a) we have three angles that are potential sources (p-source): 3, 6, 9 and three angles that are potential sinks (p-sink): 2, 5, 8. If a separatrix enters the potential source, then it turns into a saddle.

Similarly, if a separatrix starts from the potential sink, then it also turns into a saddle.

In other cases, they remain sources and sinks, respectively. Note that the separatrix cannot start in the source and go to the sink, since in this case it will be a regular curve.

Let us consider case a) in detail. Suppose there is a separatrix connecting two potential sinks, for example, 2 and 5. Then it splits the region into two parts in one of which there will be two potential sinks 6 and 9, which means there is a another separatrix that connects them or a separatrix that separates them into different area.

Thus, in this case there are at least two separatrices. Similarly, if there is a separatrix that connect to sources, then there exist an other separatrix.

Now consider the case of separatrix, that starts in a p-sink and go to a p-source. If this points are opposite (3 and 8, 2 and 6, or 5 and 9) then we obtain to polar regions. So the structure of the flow is determined by the separatrix. If the separatrix connect not opposite p-sink and p-source, then one of region contain two p-sink and two p-source and there is other separatrix in it.

In case b) we have two p-sources (4 and 9) and two p-sinks (2 and 7). In this case one separatrix is sufficient, which is given by one of the following 8 options:

1) $4 \to 9$,	3) $2 \to 7$,	5) $2 \to 4$,	7) $2 \to 9$,
2) $9 \to 4$,	4) $7 \to 2$,	6) $7 \to 4$,	8) $7 \to 9$.

In cases 1)-4) both of cells are polar, so there is by one flow structure in each of this cases. In case 5) there is the cyclic cell 4-3-2 and three possibility for elliptic angle (4, 3 or 2). By analogy, there are by three flow structure in cases 6) and 7). In case 6) we have cyclic cell 4-5-6-7 and 4 flow structures. Thus, the total number of one separatrix flow structures is

$$18 = 1(a) + 1(b1) + 1(b2) + 1(b3) + 1(b4) + 3(b5) + 4(b6) + 3(b7) + 3(b8).$$

Theorem is completed. □

2. Morse-Smale flows

Definition 2.1. *A flow X on a manifold with boundary ∂M is called a* ***Morse-Smale flow*** *if it satisfies the following conditions:*

(1) *the set of non-wandering points $\Omega(M)$ consists of finitely many of points and closed orbits and all of them are hyperbolic;*
(2) *if $u, v \in \Omega(X)$, then the unstable manifold $W^u(u)$ is transverse to the stable manifold $W^s(v)$ in $\mathrm{Int}M$;*
(3) *the restriction of X to ∂M is a Morse-Smale flow (the stable and unstable manifolds have a transversal intersection) and if $S(u)$ does not transverse $U(v)$ in M, then u or v is singular point.*

We generalize this definition to 2-dimensional stratified spaces:

Definition 2.2. ***ms-flow*** *F on a stratified space is a flow satisfying the following conditions:*

(1) *F has finitely many critical elements (fixed points and closed orbits) and all of them are non-degenerated (if a point belongs to a 0- or 1-strata then the restriction of flow to any 2-strata in the neighborhood of critical point can be extended to flow on a 2-disk with a source, saddle or sink),*
(2) *there are no saddle connections,*
(3) *α- (as well as ω-) limit set of every trajectory is a critical element.*

So each angle in a 0-strata is hyperbolic, sink or source.

The structure optimal ms-flows has the minimal number of critical elements, among all ms-flows.

Definition 2.3. *A separatrix, in the context of Morse-Smale dynamical systems, is a trajectory connecting either a saddle to a sink, or a source to a saddle and belonging to a 2-strata.*

Connections between saddles, or between a sink and a source, are forbidden in Morse-Smale systems.

Definition 2.4. *A* MS*-flow is optimal if the numbers of singular pointsand closed orbits are minimal among all* MS*-flows.*

Theorem 2.5. *Optimal* MS*-flows on the Boy's surface do not have closed orbits.*

Proof. For an optimal MS-flow on the Boy's surface, all singular points belong to the boundary, as in the example of Figure 2.1 left. In fact, this figure shows a MS-flow with 4 singular points: one of them is the 0-stratum and one on each 1-strata. Since the definition of optimal MS-flow includes the requirement of having minimal number of singular points, then an optimal MS-flow cannot have more than 4 singular points. Therefore, a system with 5 singular points (4 in the boundary and 1 in the largest 2-stratum, for example) is not optimal. Using this fact, we will prove the theorem by contradiction.

Suppose that there exists a closed orbit on the Boy's surface. By definition of an MS-flow this must be a hyperbolic cycle. It follows from the Brouwer's fixed point theorem that there exists at least one singular point in the interior of the compact region formed by this cycle. But then this singular point belongs to a 2-stratum, which adds up to 5 singular points on the whole Boy's surface (see Figure 2.1 right). This contradicts the requirement that an optimal MS-flow cannot have more than 4 singular points. Hence, there are no optimal Morse-Smale systems with closed orbits (hyperbolic cycles) on the Boy's surface. □

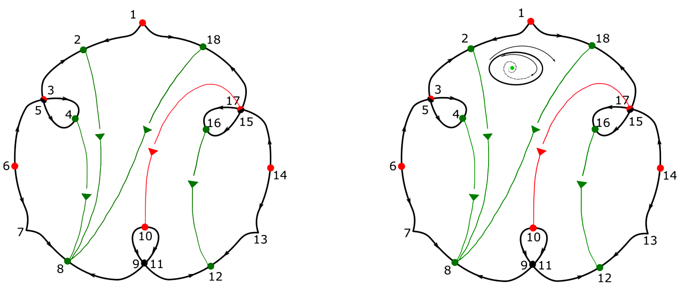

FIGURE 2.1. Optimal and non-optimal MS-flows

Theorem 2.6. *Each 1-strata of* MS*-flows contains at least one fixed point of the flow.*

Proof. We will prove it by contradiction. Suppose that the orientation in the boundary of the curved polygon in Figure 2.1 is changed such that the flow leaves point 11, go around the loop, and end at 9, *i.e.* the point 10 is regular. Then the flow goes from 9 to 8 and from 12 to 11, or vice-versa. In each case, the regular point 9/11 and the point 1 are identified together. This implies that if 10 is a regular point, then 1 must be regular as well. This is a contradiction for 1 is a 0-stratum, and thus it is a singular point. Therefore, in every loop there is at least one singular point (sink, source or saddle). □

Theorem 2.7. *Each* MS*-flow on the Boy's surface has at least* 4 *singular points: one of them is* 0*-strata and one on each* 1*-strata. Thus, every optimal* MS*-flow has* 4 *singular points. Among these flows, there are* 2 *topologically non-equivalent ones with* 8 *separatrices (*0*-strata is a source for all adjacent angles) and* 169 *flows with* 5 *separatrices (*0*-strata is a source for 5 adjacent angles and a sink for one angle). Out of these* 169 *flows,* 3 *flows have* 0 *red separatrices,* 54 *flows have* 1 *red separatrix,* 92 *flows have* 2 *red separatrices, and* 20 *flows have* 3 *red separatrices. Each flow with* 4 *singular points is topologically equivalent to one of these flows or its opposite. Thus, there are* $2 \times (2+169) = 342$ *topologically nonequivalent optimal* MS*-flows.*

Proof. By analogy with flows on closed surfaces, MS-flows on the Boy's surface are defined by the separatrix diagram. Let us first consider the case when the 0-stratum is the source for all adjoining angles (Figure 2.2 left). Since singular points lying on 1-strata have two trajectories entering them along the 1-stratum, they cannot form a red saddle with an incoming separatrix. Thus, in our case, the flow does not have red separatrices. Let us prove that such a flow has a unique sink. Suppose there are 2 sources. Then, after cutting the fundamental region along the green separatrices, due to its connectivity, a region will be formed that has 2 sinks on the boundary. Then they must be separated by a red separatrix, which is impossible. The resulting contradiction proves the existence of a unique sink. There are two different possibilities for choosing such a point – these are points 2 and 4. Flows with sinks at points 5, 8, 12, 14 and 18 are obtained from a flow with sink at 2 by symmetries and rotations of the pattern by $2\pi/3$. So there are 2 topologically non-equivalent flows in this case, (Figures 2.3-1 and 2.3-2)

Let us now consider flows with directed trajectories on 1-strata shown in Figure 2.2 right. Since there are only 3 red points (6, 10 and 14) on

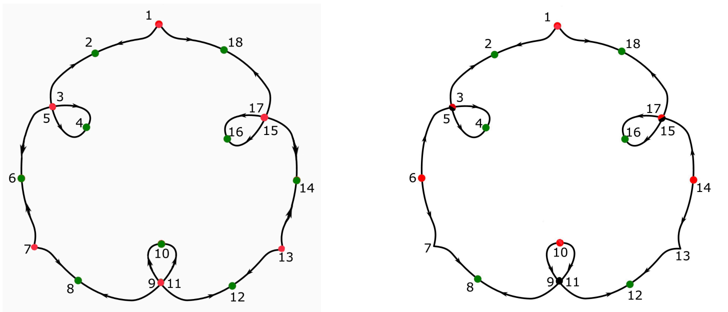

FIGURE 2.2. Possible orientations of optimal MS-flows in the boundary

1-strata, only they can be saddles of red separatrices. Thus, the number of red separatrices does not exceed 3.

We begin our consideration of such flows with flows without red separatrices (Figure 2.3-11). In this case, considering the arguments as above, there is only one sink. It can be one of points 2, 4 or 8. The remaining 3 points (12, 16, 18) give symmetrical flows with respect to the first 3. Hence, there are 3 topologically non-equivalent flows without red separatrices.

Consider now the case of one red separatrix. It can end at the saddle 6 or 10 (case 14 is symmetrical to 6). Let the separatrix end at 6. If at the same time it starts at 3 ($3 \to 6$, see Figure 2.3-5), then 4 is a sink, and in another area into which it divides the diagram, the remaining green points can be sinks: 2, 8, 12, 16, 18. So there are 5 different threads in this case.

If the separatrix starts at 1 ($1 \to 6$, Figure 2.3-3), it divides the area into two parts with two $(2, 4)$ and four $(8, 12, 16, 18)$ points that can be sinks, thus $2 \times 4 = 8$ options in total. In case $17 \to 6$ (Figure 2.3-7), we have $3 \times 3 = 9$ options, $14 \to 6$ (Figure 2.3-4) gives $4 \times 2 = 8$ options, and case $10 \to 6$ (Figure 2.3-6) gives $5 \times 1 = 5$ options.

If the red separatrix ends at 10, then possible axial symmetries of the diagrams must be taken into account. Thus, for example, all options with $6 \to 10$ are symmetrical to the corresponding options with $14 \to 10$. Therefore, we will consider only one of them. For $14 \to 10$ (Figure 2.3-8) we have $1 \times 5 = 5$ options, for $17 \to 10$ (Figure 2.3-9) we have $2 \times 4 = 8$ options, and for $1 \to 10$ (Figure 2.3-10) there will be 6 different non-symmetrical options (2-18, 2-16, 2-12, 4-16, 4-12, and 8-12). Summing up all these numbers, we get $5 + 8 + 9 + 8 + 5 + 5 + 8 + 6 = 54$ variants with one red separatrix.

We now turn to the case with two red separatrices. Red saddles can be 6 and 10 or 6 and 14 (the case of 10 and 14 is symmetrical to 6 and 10). In this case, the number of variants will be equal to the product of the numbers of saddles lying in three parts into which two red sepraartris divide

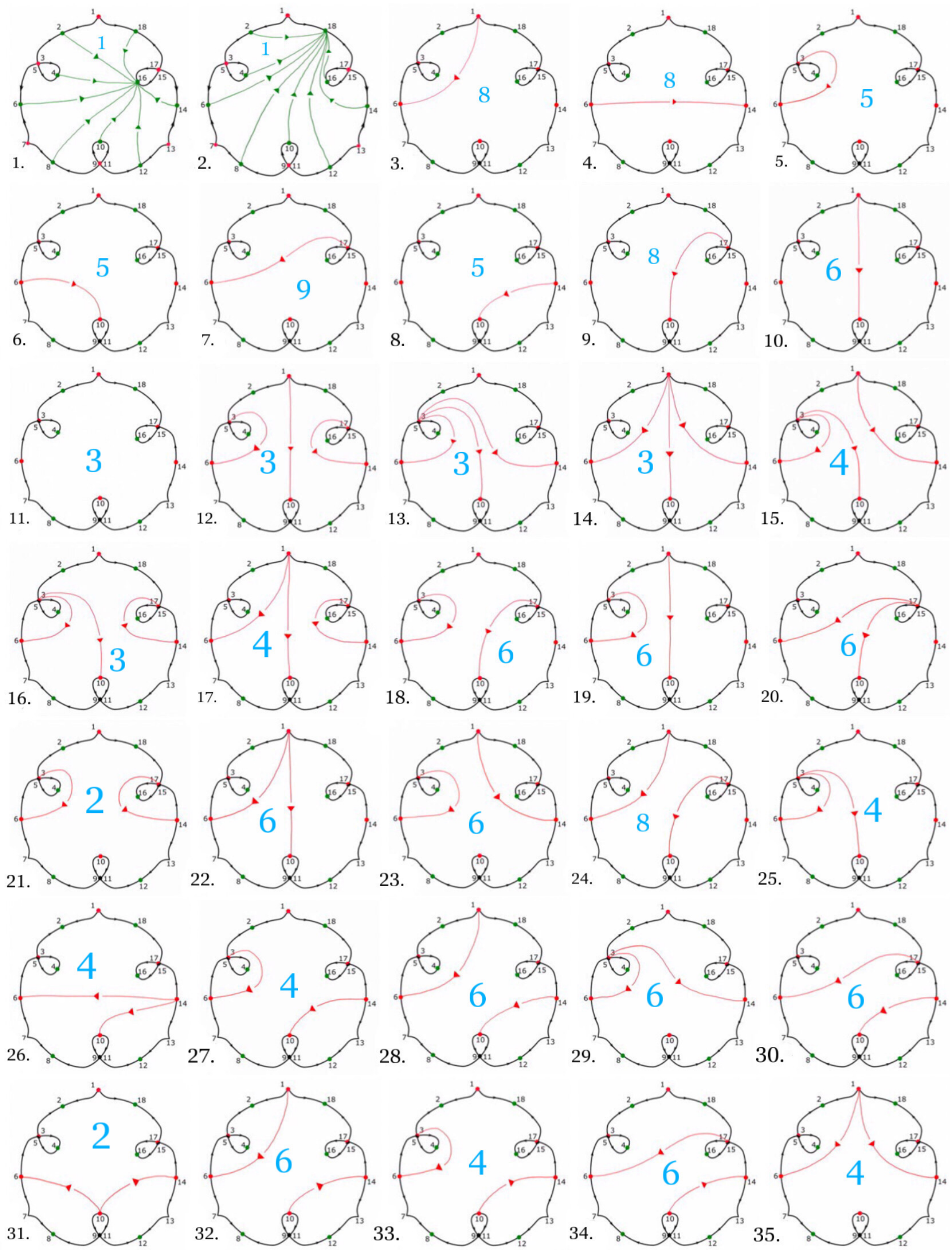

FIGURE 2.3. Optimal Morse-Smale flows on the Boy's surface

the diagram. For example, for $1 \to 6$ and $1 \to 10$ in one part there are two saddles 2 and 4, in the other one 8, and in the third three $(12, 16, 18)$. We get, $2 \times 1 \times 3 = 6$ options. Let us describe all possible variants with two separatrices:

$$
\begin{array}{rll}
1) & 3 \to 6, 3 \to 10 \ \ \text{(see Figure 2.3-25)}: & 1 \times 1 \times 4 = 4 \\
2) & 3 \to 6, 1 \to 10 \ \ \text{(see Figure 2.3-19)}: & 1 \times 2 \times 3 = 6 \\
3) & 3 \to 6, 17 \to 10 \ \ \text{(see Figure 2.3-18)}: & 1 \times 3 \times 2 = 6 \\
4) & 3 \to 6, 14 \to 10 \ \ \text{(see Figure 2.3-27)}: & 1 \times 4 \times 1 = 4 \\
5) & 1 \to 6, 1 \to 10 \ \ \text{(see Figure 2.3-22)}: & 2 \times 1 \times 3 = 6 \\
6) & 1 \to 6, 17 \to 10 \ \ \text{(see Figure 2.3-24)}: & 2 \times 2 \times 2 = 8 \\
7) & 1 \to 6, 14 \to 10 \ \ \text{(see Figure 2.3-32)}: & 2 \times 3 \times 1 = 6 \\
8) & 17 \to 6, 17 \to 10 \ \ \text{(see Figure 2.3-20)}: & 3 \times 1 \times 2 = 6 \\
9) & 17 \to 6, 14 \to 10 \ \ \text{(see Figure 2.3-30)}: & 3 \times 2 \times 1 = 6 \\
10) & 14 \to 6, 14 \to 10 \ \ \text{(see Figure 2.3-26)}: & 4 \times 1 \times 1 = 4 \\
11) & 3 \to 6, 3 \to 14 \ \ \text{(see Figure 2.3-29)}: & 1 \times 2 \times 3 = 6 \\
12) & 3 \to 6, 1 \to 14 \ \ \text{(see Figure 2.3-23)}: & 1 \times 3 \times 2 = 6 \\
13) & 3 \to 6, 17 \to 14 \ \ \text{(see Figure 2.3-21)}: & 1 \times 2 \times 3 = 2 \\
14) & 3 \to 6, 10 \to 14 \ \ \text{(see Figure 2.3-33)}: & 1 \times 4 \times 1 = 4 \\
15) & 1 \to 6, 1 \to 14 \ \ \text{(see Figure 2.3-35)}: & 1 \times 2 \times 2 = 4 \\
16) & 1 \to 6, 10 \to 14 \ \ \text{(see Figure 2.3-32)}: & 1 \times 2 \times 3 = 6 \\
17) & 17 \to 6, 10 \to 14 \ \ \text{(see Figure 2.3-34)}: & 1 \times 2 \times 3 = 6 \\
18) & 10 \to 6, 10 \to 14 \ \ \text{(see Figure 2.3-31)}: & 1 \times 2 \times 1 = 2
\end{array}
$$

Summing up all the numbers we get 92 options.

Similarly, one can consider cases with three separatrices, and get the following description:

$$
\begin{array}{rll}
1) & 3 \to 6, 3 \to 10, 3 \to 14 \ \ \text{(see Figure 2.3-13)}: & 1 \times 1 \times 1 \times 3 = 3 \\
2) & 3 \to 6, 3 \to 10, 1 \to 14 \ \ \text{(see Figure 2.3-15)}: & 1 \times 1 \times 2 \times 2 = 4 \\
3) & 3 \to 6, 3 \to 10, 17 \to 14 \ \ \text{(see Figure 2.3-16)}: & 1 \times 1 \times 3 \times 1 = 3 \\
4) & 3 \to 6, 1 \to 10, 1 \to 14 \ \ \text{(see Figure 2.3-17)}: & 1 \times 1 \times 2 \times 2 = 4 \\
5) & 3 \to 6, 1 \to 10, 17 \to 14 \ \ \text{(see Figure 2.3-12)}: & 1 \times 1 \times 3 = 3 \\
6) & 1 \to 6, 1 \to 10, 1 \to 14 \ \ \text{(see Figure 2.3-14)}: & 1 \times 1 \times 3 = 3
\end{array}
$$

Summing up all the numbers we get 20 options.

By changing the direction of movement along closed trajectories, we obtain the same numbers of topologically non-equivalent flows. In total, we have $2 \times 2 = 4$ flows with 8 separatrices and $2 \times (3 + 54 + 92 + 20) = 338$ flows with 5 separatrices. $\square$

3. Projective MS-flow

In this section we consider Morse-Smale flows on the real projective plane, which are flows projected on the Boy's surface. PMS-flows have similar properties to MS-flow, but in addition PMS-flows are symmetric in the neighborhoods of fixed point.

Hyperbolic singular points on the Boy's surface must keep their type when extended to the real projective plane. In other words, a sink point in one of the strata of the Boy's surface must still be a sink on the projective plane, and the same holds for sources and saddles. This implies that PMS-flows are central symmetric near singular points. As a consequence, the only possible boundary orientation is a symmetric one, shown in Figure 2.2 left. In it, we have this identification of each point:

$$2 = 12, \qquad 6 = 14, \qquad 8 = 18,$$
$$1 = 9 = 11, \qquad 13 = 3 = 5, \qquad 7 = 15 = 17.$$

Points 4, 10 and 16 are either sink (for every 2-strata) or saddle (for every 2-strata), since these are inner points on the projective plane.

Of course, the boundary orientation in which all the potential sources are potential sinks, and vice-verse, is also possible, but the results will be similar.

Theorem 3.1. *Each optimal* PMS*-flow on the projective plane has* 3 *sources,* 5 *saddles, and* 3 *sinks. There exist* $80 = 2 \times (1 + 9 + 30)$ *optimal* PMS*-flows.*

Proof. Figure 3.1 shows each step used in the process of counting all 40 PMS-flows. Again, the boundary orientation in which red points are green points, and vice-versa, gives the other 40 PMS-flows, adding up to 80 in the end.

The first portrait shows the case in which 4, 16 are saddles, and 10 is a sink. This is the only possibility of green separatrices, up to symmetry, for optimal PMS-flow.

When 4, 16 are sinks, and 10 saddle, there will necessarily be a saddle (yellow point) inside the largest 2-stratum. This is represented in the second and third portraits. The dashed red lines are the possible red separatrices. We have 6 cases in the first portrait and 3 in the second, *i.e.* 9 cases.

The remaining portraits present the situation in which 4, 10, 16 are sinks. There will be two saddles inside the largest 2-stratum. Counting all

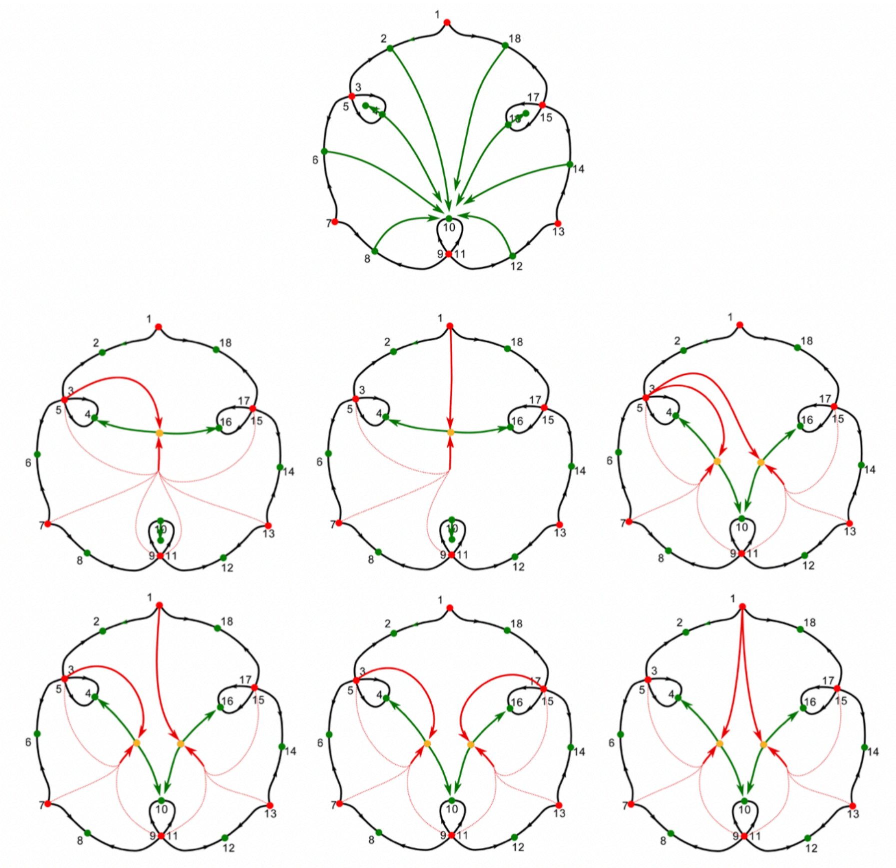

Figure 3.1. Optimal pms-flows

the possibilities of red separatrices: $9+9+6+6=30$. Notice that the two last portraits have 3 symmetrically equal flows each.

Suppose a trajectory leaves the 0-stratum. Then, since the optimal projective flow is symmetric at fixed points, the 0-stratum is a source for all angles in it. Each 1-stratum has one fixed point of the p-sink (potential sink). Let us enumerate the corners as in Figure 2.2 left. Inside each 2-disk the following two types of flow are possible: with a sink inside or with a sink at the boundary (in the p-sink). The 0-stratum corresponds to three points on the projective plane. Therefore, the flow will have at least three sources. Since there must be a sink on each 2-disk, there are also at least 3 sinks.

Further we will show the existence of flows with three sources and three sinks. Since the Euler characteristic of the projective plane is equal to 1 and is equal to the sum of the number of sources and sinks minus the number of saddles, the optimal flow has three sources, three sinks and five saddles. If all the sinks of the 2-disks are internal, then the central region must also have a sink, and therefore such a flow will not be optimal.

Let only one disk have a sink at the boundary. For definiteness, assume that its index is 10. Then a unique structure of such a flow is possible. In this case, all green separatrices end at 10.

Next, consider the case of two sinks at the boundary. Assume that their indexes are 4 and 16. For such flows there possible an axial symmetry transforming 4 into 16. These points should be separated by red separatrices. Since all red points on the border are sources, there is a saddle inside the central region. The two separatrices that enter into that region start at points that lay on opposite sides of points 4 and 16. Then one of them is 1, 3, or 17, and the other is 5, 7, 9, 11, 13 or 15. If the first is 1, then 5, 7, 9 are symmetric to 15, 13, 11, respectively. In other words, there are only three different structures of such flows. Since 3 is symmetric to 17, we will consider only the options of separatrices starting at 3. For the second separatrix, 6 options are possible, and thus we have 6 more flow structures.

Now we consider the case of three sinks at the boundaries of 2-disks, that is, when points 4, 10, and 16 are sinks. In this case, there are two saddles inside the central area. Their stable manifolds (red separatrices) are separated by points 4, 10, and 16. There are 30 structures of such type. To see this, we introduce the concept of saddle weight. The stable manifold of the saddle splits the central region into two parts. The weight is equal to the number of saddles +1 of the part in which there is one sink.

In view of the symmetries, we can assume that these regions for a pair of saddles contain sinks 4 and 16 and the weight of the saddle adjacent to the first region (with sink 4) is not greater than the weight of the second saddle. Then the numbers of structures for distinct weights is given in the following Table 3.1. In total we get 30 structures. □

weights	number of structures	weights	number of structures	weights	number of structures
$1,1$	1	$2,2$	3	$3,4$	3
$1,2$	2	$2,3$	5	$3,5$	1
$1,3$	3	$2,4$	3	$4,4$	1
$1,4$	2	$2,5$	1		
$1,5$	1	$3,3$	4		

Table 3.1.

Conclusions

It is known that there is a unique optimal Morse-Smale flow on the projective plane and it has 3 fixed points: one source, one sink and one saddle. We have shown that the condition that the flow is projected into a flow on the Boy's surface increases the number of fixed points to 11, and the possible flows themselves to 80. If the Boy's surface is considered as a stratified set, then there are even more optimal flows, namely, 342. But if we do not impose Morse-Smale conditions, then there are only 18 optimal flows. A remained interesting problem consists of describing of all possible extensions of the constructed PMS-flows to optimal flows on a three-dimensional sphere, as well as describing optimal flows for immersions of other surfaces.

References

[1] A. Andronov, L. Pontryagin. Rough systems. *Doklady Akademii Nauk SSSR*, 14(5):247–250, 1937.

[2] Werner Boy. Über die Curvatura integra und die Topologie geschlossener Flächen. *Math. Ann.*, 57(2):151–184, 1903, doi: 10.1007/BF01444342.

[3] O. A. Giryk. Classification of polar Morse-Smale vector fields on two-dimensional manifolds. *Methods Funct. Anal. Topology*, 2(1):23–37, 1996.

[4] S. Goodman, M. Kossowski. Immersions of the projective plane with one triple point. *Differential Geometry and Its Applications*, 27(4):527–542, 2009, doi: 10.1016/j.difgeo.2009.01.011.

[5] O.A. Kadubovskyj. Classification of morse-smale vector fields on 2-manifolds. *Visn., Mat. Mekh., Kyïv. Univ. Im. Tarasa Shevchenka*, 14:85–88, 2005.

[6] Z. Kibalko, O. O. Prishlyak, R. Shchurko. Trajectory equivalence of optimal Morse flows on closed surfaces. *Proc. Int. Geom. Cent.*, 11(1):12–26, 2018, doi: 10.15673/tmgc.v11i1.916.

[7] Rob Kusner. Conformal geometry and complete minimal surfaces. *Bull. Amer. Math. Soc. (N.S.)*, 17(2):291–295, 1987, doi: 10.1090/S0273-0979-1987-15564-9.

[8] E. Leontovich, A. Mayer. On a scheme determining the topological structure of the separation of trajectories. *Dokl. Akad. Nauk SSSR (N.S.)*, 103:557–560, 1955.

[9] Sergiy Maksymenko. Local inverses of shift maps along orbits of flows. *Osaka J. Math.*, 48(2):415–455, 2011, http://projecteuclid.org/euclid.ojm/1315318347.

[10] A. G. Mayer. Rough transformations of the circle to the circle. *Uch. Zap. GGU*, 12:215–229, 1939.

[11] Bernard Morin. Équations du retournement de la sphère. *C. R. Acad. Sci. Paris Sér. A-B*, 287(13):A879–A882, 1978.

[12] A. A. Oshemkov, V. V. Sharko. On the classification of Morse-Smale flows on two-dimensional manifolds. *Mat. Sb.*, 189(8):93–140, 1998, doi: 10.1070/SM1998v189n08ABEH000341.

[13] J. Palis, S. Smale. Structural stability theorems. In *Global Analysis (Proc. Sympos. Pure Math., Vol. XIV, Berkeley, Calif., 1968)*, pages 223–231. Amer. Math. Soc., Providence, R.I., 1970.

[14] M. M. Peixoto. On structural stability. *Ann. of Math. (2)*, 69:199–222, 1959, doi: 10.2307/1970100.

[15] M. M. Peixoto. Structural stability on two-dimensional manifolds. *Topology*, 1:101–120, 1962, doi: 10.1016/0040-9383(65)90018-2.

[16] M. M. Peixoto. On the classification of flows on 2-manifolds. In *Dynamical systems (Proc. Sympos., Univ. Bahia, Salvador, 1971)*, pages 389–419, 1973.

[17] O. O. Prishlyak. Morse-Smale vector fields without closed trajectories on three-dimensional manifolds. *Mat. Zametki*, 71(2):254–260, 2002, doi: 10.1023/A:1013963315626.

[18] O. O. Prishlyak. Topological equivalence of Morse-Smale vector fields with beh 2 on three-dimensional manifolds. *Ukraïn. Mat. Zh.*, 54(4):492–500, 2002, doi: 10.1023/A:1021035327909.

[19] O. O. Prishlyak. On the sum of indices of flow with isolated singular points on a stratified set. *Mat. Fiz. Anal. Geom.*, 10(1):106–115, 2003.

[20] O. O. Prishlyak. Topological classification of m-fields of two- and three-dimensional manifolds with boundary. *Ukrainian Mathematical Journal*, 55(6):799–805, 2003, doi: 10.1023/B:UKMA.0000010596.67853.89.

[21] O. O. Prishlyak. Complete topological invariants of morse-smale flows and handle decompositions of 3-manifolds. *J. Math. Sci., New York*, 144(5):4492–4499, 2007, doi: 10.1007/s10958-007-0287-y (in English).

[22] O. O. Prishlyak, M. V. Loseva. Topology of Morse-Smale flows with singularities on the boundary of a two-dimensional disk. *Proc. Int. Geom. Cent.*, 9(2):32–41, 2016.

[23] O. O. Prishlyak, M. V. Loseva. Optimal Morse-Smale flows with singularities on the boundary of surface. *J. Math. Sci., New York*, 243(2):279–286, 2019, doi: 10.1007/s10958-019-04539-9 (in English).

[24] O. O. Prishlyak, A. Prus, S. Guraka. Flows with collective dynamics on a sphere. *Proc. Int. Geom. Cent.*, 14(1):61–80, 2021, doi: 10.15673/tmgc.v14i1.1902 (in English).

[25] O. O. Prishlyak, A. A. Prus. Morse-Smale flows on a torus with a hole. *Proc. Int. Geom. Cent.*, 10(1):47–58, 2017.

[26] O. O. Prishlyak, A. A. Prus. A three-color graph of Morse flow and a compact surface with a boundary. *Nonlinear Oscillations*, 22(2):250–261, 2019, doi: 10.12697/acutm.2018.22.22.

[27] Stephen Smale. Morse inequalities for a dynamical system. *Bull. Amer. Math. Soc.*, 66:43–49, 1960, doi: 10.1090/S0002-9904-1960-10386-2.

Received: March 3, 2022, accepted: April 28, 2022.

Alexandr Prishlyak
Taras Shevchenko National University of Kyiv, Faculty of Mechanics and Mathematics, 4th Academician Glushkov avenue, Kyiv, 03127, Ukraine
Email: prishlyak@yahoo.com
ORCID: 0000-0002-7164-807X

Luca Di Beo
Taras Shevchenko National University of Kyiv, Faculty of Mechanics and Mathematics, 4th Academician Glushkov avenue, Kyiv, 03127, Ukraine
Email: dibeoluca@gmail.com